Supplementary Information (SI) for CrystEngComm.

Supporting Information for

Boosting Oxygen Evolution Activity via Cr-Induced Electronic and Structural Modulation in NiFe-LDH Nanosheets

Yinfeng Wang[a,b,‡], Yuhao Zhou[a,‡], Yangchun Guo[a,b], Xuan Zhao[a,b], Zhenhong He[b,*], Shufang Ma[a], Bingshe Xu[a,c], Xiaodong Hao[a,*]

[a]*Xi'an Key Laboratory of Compound Semiconductor Materials and Devices, School of Physics & Information Science, Shaanxi University of Science & Technology, Xi'An 710021, China*

[b]*Shaanxi Key Laboratory of Chemical Additives for Industry, College of Chemistry and Chemical Engineering, Shaanxi University of Science & Technology, Xi'an 710021, China*

[c]*Key Laboratory of Interface Science and Engineering in Advanced Materials, Ministry of Education, Taiyuan University of Technology, Taiyuan, 030024, China*

*Corresponding author: hao.xiaodong@sust.edu.cn; hezhenhong@sust.edu.cn

Experimental Section

Chemicals and Materials. The following chemicals were used in this experiment: nickel(II) nitrate hexahydrate ($Ni(NO_3)_2 \cdot 6H_2O$), iron(III) nitrate nonahydrate ($Fe(NO_3)_3 \cdot 9H_2O$), chromium(III) chloride hexahydrate ($CrCl_3 \cdot 6H_2O$), urea ($CO(NH_2)_2$), ammonium fluoride (NH_4F), and potassium hydroxide (KOH). All reagents were of analytical grade and used without further purification.

Synthesis of Materials. NiFeCr-LDHs were synthesized according to the following procedure. First, predetermined amounts of $Ni(NO_3)_2 \cdot 6H_2O$, $Fe(NO_3)_3 \cdot 9H_2O$, and $CrCl_3 \cdot 6H_2O$ were dissolved in 40 mL of deionized water contained in a beaker. The total concentration of metal cations was fixed at 2.5 mmol, and the molar ratio of Ni:(Fe + Cr) was maintained at 4:1. While stirring, 12.5 mmol of urea and 3.5 mmol of NH_4F were added to the solution. The mixture was subsequently stirred vigorously using a magnetic stirrer for 30 minutes. The resulting mixture was then transferred into a 70 mL Teflon-lined autoclave and heated in a homogeneous reactor at 120 °C for 8 hours. After natural cooling to room temperature, the product was collected and washed several times with ethanol and deionized water, respectively. The washed solid was dried in a vacuum oven at 60 °C for 6 hours, and the final product was labeled as NiFeCr-LDHs. By varying the Fe:Cr molar ratio while keeping the remaining experimental steps unchanged, a series of samples were prepared. Specifically, when the Fe:Cr ratios were set to 7:1, 3:1, 5:3, and 1:1, the corresponding samples were designated as NiFeCr-1, NiFeCr-2, NiFeCr-3, and NiFeCr-4, respectively. For comparison, a reference sample labeled NiFe-LDH was also prepared under the condition of a Ni: Fe molar ratio of 4:1.

Materials Characterization. The crystal structure of the powder samples was determined by X-ray powder diffraction (XRD) analysis using a Rigaku D/MAX-2500/pc diffractometer. X-ray photoelectron spectroscopy (XPS) measurements were conducted at the KBSI Daeduk Center with a Kratos AXIS Ultra spectrometer. For electron microscopy characterization, a 10 μL aliquot of the redispersed sample was drop-cast onto a carbon film approximately 5 nm thick. Low-magnification transmission electron microscopy (TEM) images were acquired using a JEM-2100Plus (JEOL) microscope operated at an accelerating voltage of 200 kV. Aberration-corrected scanning transmission electron microscopy (STEM) characterization was performed using a JEM-ARM 300F microscope equipped with probe and image correctors and a cold field emission gun, operated at 300 kV. The probe convergence semi-angle was approximately 24.5 mrad. Annular bright-field (ABF) and high-angle annular dark-field (HAADF) images were collected with angular ranges of 11–22 mrad and 54–220 mrad, respectively. Elemental analysis was carried out using energy-dispersive X-ray spectroscopy (EDS) with a dual-EDS system (JED-2300T) featuring two large-area, windowless silicon drift detectors. The total solid angle for EDS collection was 2.2 sr. Furthermore, electron energy loss spectroscopy (EELS) was performed using a Gatan camera system (GIF Quantum ER Model 965) to obtain valence state information of the samples. The EPR measurement was performed on a Bruker Emxplus instrument from Bruker Corporation, Germany.

Electrochemical Measurements. All electrochemical tests were conducted at room temperature (25 ± 1 °C) using a CHI660D electrochemical workstation. A standard three-electrode system was employed, consisting of a glassy carbon working electrode (3 mm in diameter), a graphite rod counter electrode, and an Hg/HgO reference electrode. Electrode activation was performed by linear sweep voltammetry at a scan rate of 5 mV s^{-1}, sweeping from 0 V to −2 V versus the Hg/HgO reference electrode. Electrochemical impedance spectroscopy (EIS) was used to investigate electrode kinetics and interfacial charge transfer resistance. All EIS data were acquired at a constant potential of 1.50 V versus the reversible hydrogen electrode (RHE), with a sinusoidal perturbation amplitude of 5 mV over a frequency range from 100 kHz to 0.1 Hz. Before each measurement, the working electrode was pre-stabilized at this potential for 60 s to allow the reaction current to reach a steady state, thereby avoiding transient effects on the impedance response. To accurately characterize the electrochemical polarization, all steady-state polarization curves were corrected with 85% iR compensation to eliminate the influence of the ohmic drop in solution. The potentials recorded versus the Hg/HgO reference electrode were converted to the RHE scale using the Nernst equation. The conversion follows the equation below:

$$E_{RHE} = E_{Hg/HgO} + 0.0592 \times pH + 0.098\,V\ (25℃)$$

where $E_{Hg/HgO}$ is the standard potential of the Hg/HgO electrode at 25 °C.

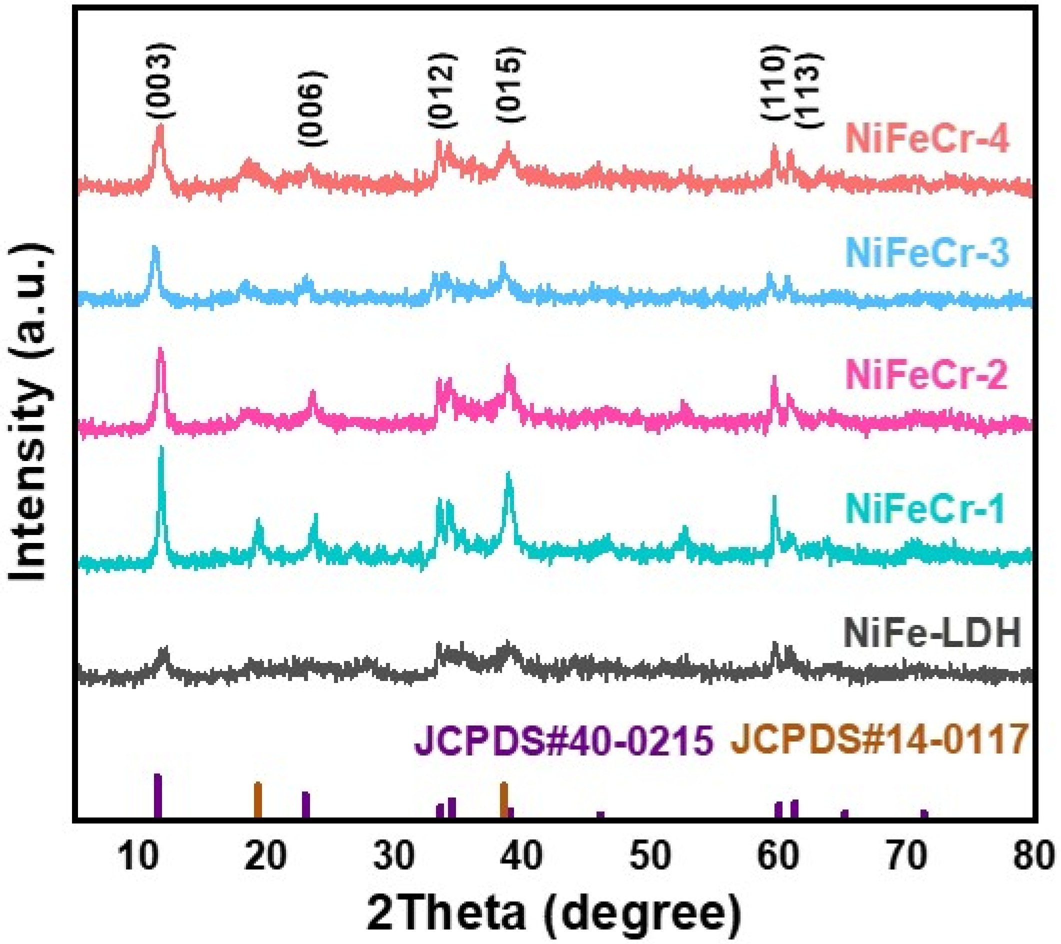

Fig. S1 XRD patterns of the as-prepared NiFe-LDH and NiFeCr-LDHs samples.

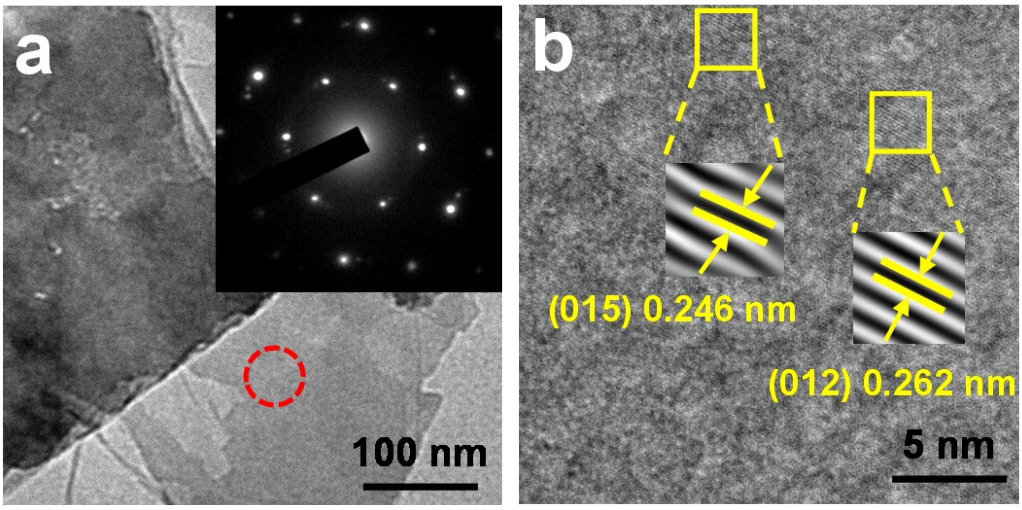

Fig. S2 TEM images of the prepared NiFe-LDH samples. The corresponding SAED pattern for the NiFe-LDH sample is provided in the inset.

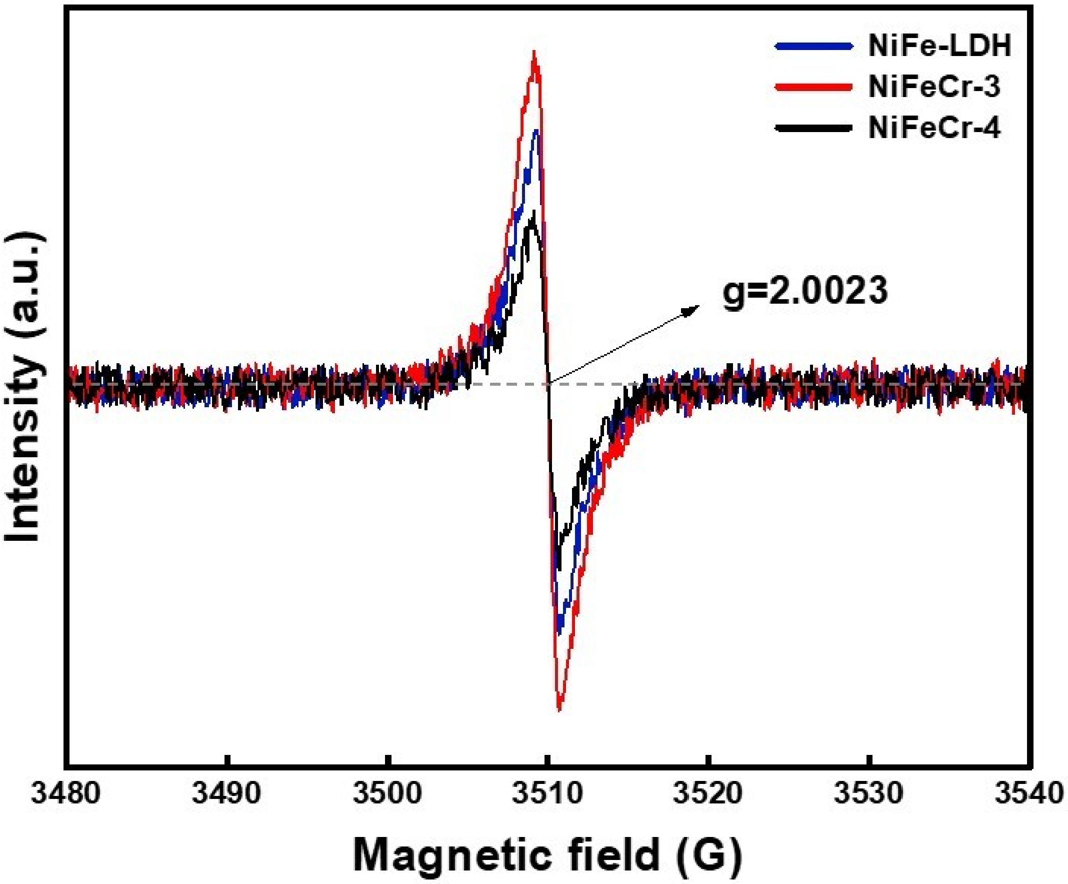

Fig. S3 EPR spectra of NiFe-LDH, NiFeCr-3, and NiFeCr-4 nanosheets.

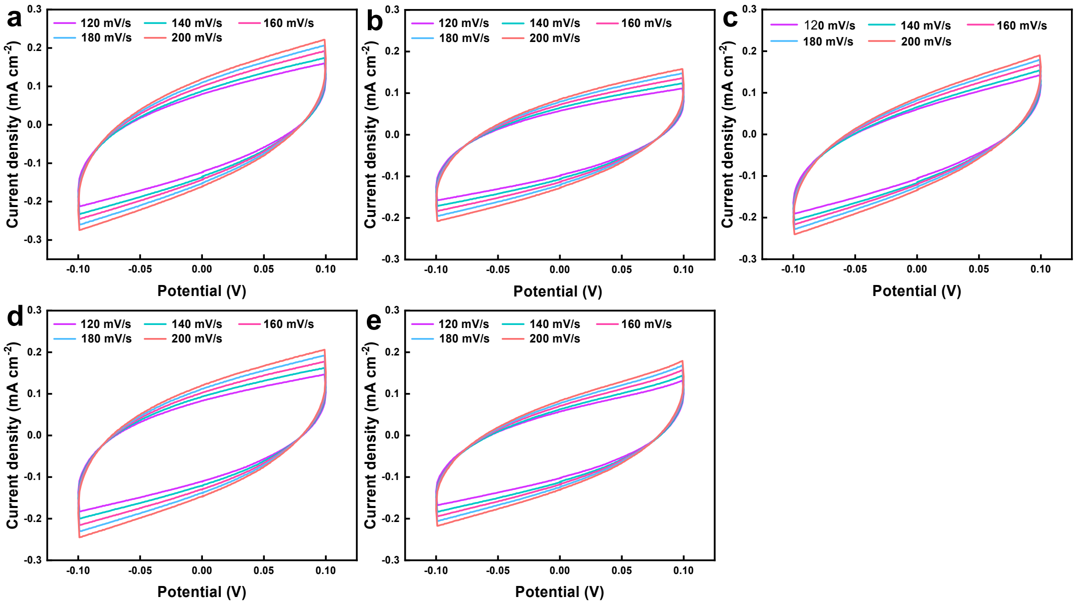

Fig. S4 Cyclic voltammetry curves of (a) NiFe-LDH (b) NiFeCr-1 (c) NiFeCr-2 (d) NiFeCr-3 (e) NiFeCr-4 at different scan rates for OER.

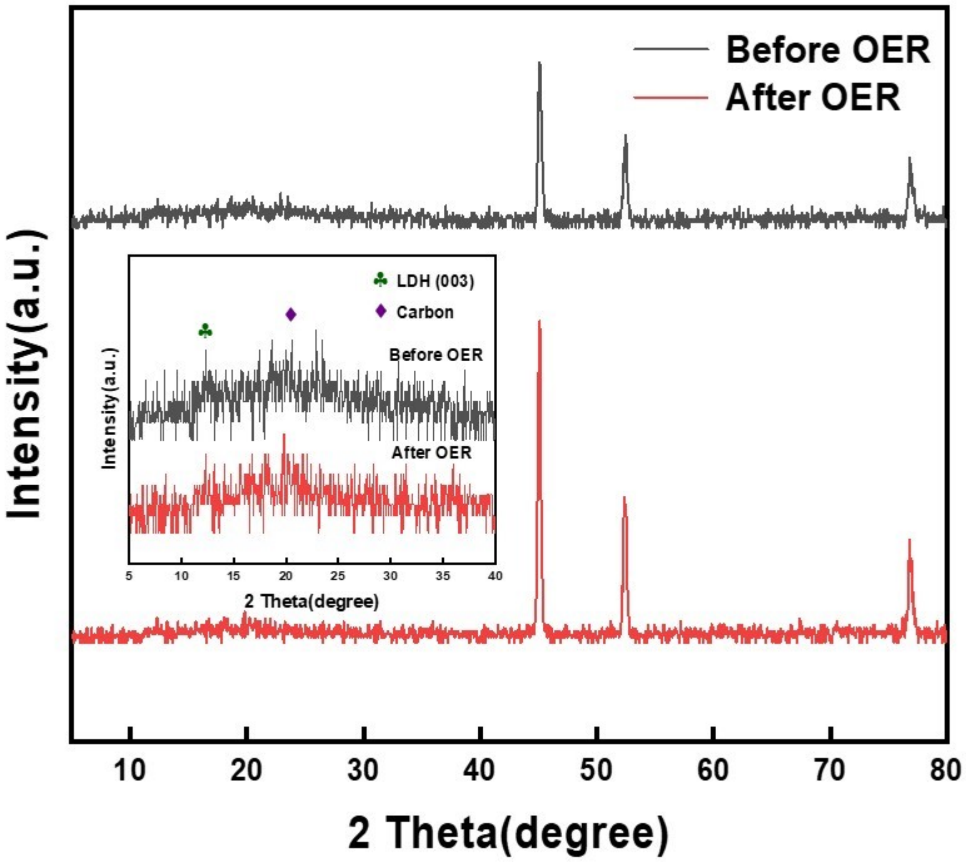

Fig. S5 XRD patterns of nickel foam loaded with 0.5 mg carbon black and 2.5 mg catalyst before and after the electrocatalytic reaction.

Table S1 Comparison of OER performance for NiFeCr-3 with recently reported transition-metal-based electrocatalysts in alkaline electrolyte.

Catalysts	**η_{100} (mV)**	**Electrolyte**	**References**
NiFeCr-3	**331**	**1 M KOH**	**This work**
Cr-CoXP	334	1 M KOH	Adv. Funct. Mater. 33 (2023)2214081.
CrxNi$_1$−xSe$_2$/CC$_b$	400	1 M KOH	Nano Res. 17 (3) (2024)1199-1208.
Ni$_3$S$_4$@Ni(OH)$_2$	356	1 M KOH	J. Colloid Interf Sci. 654 (2024) 66002D75.
NiMoO$_4$-S/Ni$_3$S$_2$/NF	355	1 M KOH	J. Alloys Compd. 970 (2024) 172530.
CoFeGaNiZn	370	1 M KOH	Nano Res.15 (2021) 4799–4806.
FeCoNi alloy	400	1 M KOH	Chemistry Select. 2 (2017) 1630-1636.
FeNiMnCrCu	342	1 M KOH	Hydrog. Energy. 47 (2022) 31330–31341.
Ni SAs@S/N-FCS	335	1 M KOH	Angew. Chem. Int. Ed. 61 (2022) 202212542.
CoFe/CoFe$_2$O$_4$@NC	370	1 M KOH	Chem. Eng. J. 523 (2025) 168363.
FeCoMnCuAl	370	1 M KOH	Prog. Nat. Sci.:Mater. Int. 34 (2024) 880.
NiFe-PBA-gel-cal	340	1 M KOH	Adv. Sci. 9 (2022) 2200146.
Ni$_{4/5}$Fe$_{1/5}$-LDHs-S-2	346	1 M KOH	Chin. J. Catal. 41 (2020) 847.
NF-C/CoS/NiOOH	361	1 M KOH	Nano-Micro Lett. 12 (2020) 162.